RSC Advances

ROYAL SOCIETY OF CHEMISTRY

www.rsc.org/advances

Preparation and in vitro cell-biological performance of sodium alginate/nano-zinc silicate co-modified calcium silicate bioceramics

Kun Xiong[a,b,c,#], Jing Zhang[a,b,#], Haishan Shi[a,b], Jingqun Liu[a,b], Huae Wu[a,b], Haiyan Li[a,b], Jiandong Ye[a,b,*]

[a] School of Materials Science and Engineering, South China University of Technology Guangzhou 510640, China

[b] National Engineering Research Center for Tissue Restoration and Reconstruction, Guangzhou 510006, China

[c] State Key Laboratory Cultivation Base for Nonmetal Composites and Functional Materials, Southwest University of Science and Technology, Mianyang 621010, China

[*] Author to whom correspondence should be addressed. e-mail: jdye@scut.edu.cn; quentin83@126.com; Tel: +86(20)22236283; Fax: +86(20)22236088

[#] Kun Xiong and Jing Zhang contribute equally to the first author.

Abstract:

Sodium alginate/nano-zinc silicate (SA/nano-ZS) co-modified calcium silicate bioceramics (Na/Zn-CS) were prepared via the spin-coating process. X-ray diffraction patterns indicated, the surface components of Na/Zn-CS disks were composed of calcium silicate (pseudowollastonite, CS), sodium calcium silicate and Na/Ca co-doped zinc silicate. Na/Zn-CS disks could induce hydroxyapatite to rapidly deposit on the surface of the disks after being soaked in simulated body fluid (SBF). The pH value of SBF, in which Na/Zn-CS disks were soaked, remained in a relative low range, whereas that of SBF, in which pure CS disks were soaked, increased with the prolongation of soaking time. Whether rat bone marrow mesenchymal stem cells (rBMSCs) were co-cultured with CS disks or with Na/Zn-CS disks, the extracellular matrix mineralization of rBMSCs could be observed, which suggests the released silicon from the samples possesses osteoinductivity. F-actin staining images of rBMSCs revealed that the attachment and the spread of rBMSCs would not be influenced by the inorganic ions released from the samples, but by the interface stability of cell/material. Furthermore, the surface dissolution rate significantly affected the initial proliferation of rBMSCs. After incubation for 14 days, the alkaline phosphatase (ALP) activity of rBMSCs cultured on the surface of CS disk spin-coated with 0.1 g/mL of SA/nano-ZS suspension (Na/0.1Zn-CS) was much higher than that of rBMSCs cultured on the surface of pure CS disk, which indicates the released zinc ions can promote the differentiation of rBMSCs. In conclusion, the surface co-modification with SA/nano-ZS is an effective way to improve the dissolution behavior and biological performance of CS bioceramics.

Keywords: zinc silicate, sodium alginate, calcium silicate, surface modification, rBMSCs.

1. Introduction

Calcium silicate were widely used as bioceramics, coatings and additives owing to their excellent biocompatibility, superior bioactivity and good biomineralization ability [1-8]. Pseudowollastonite phase calcium silicate (CS) bioceramic not only have higher mechanical property than bioglass, but also show better bioactivity than the stoichiometric hydroxyapatite (HA) bioceramics. Because of its ability to release silicate ions, CS bioceramics also possess osteoinductivity, whereas calcium phosphate based biomaterials do not have such ability[9]. Silicon is one of the vital trace elements in human bone, and it plays an important role in bone formation and bone regeneration [10-12]. Silicate ions can affect osteoblast behavior and further accelerate the restoration of bone tissue. What's more, silicate ions also have the ability to up-regulate the osteogenic-related gene expressions in osteoblast [13, 14]. When calcium silicate degrades, sianols (Si-OH) will form and provide the active sites for the deposition of apatite, which facilitates the calcification of bone matrix [15, 16]. In addition, calcium silicate is capable to induce angiogenesis, which benefits for the bone regeneration [17-19].

However, the overhigh dissolution rate of CS will cause high pH value in the surrounding area, which restricts their further biological or medical applications [20]. Currently, ion doping is an effective way to control the high dissolution rate of CS. But when calcium atom is substituted by other atoms to a certain degree, the phase will change, and the solid solution such as hardystonite ($Ca_2ZnSi_2O_7$) [20, 21], akermanite ($Ca_2MgSi_2O_7$) [22-24], diopside ($CaMgSi_2O_6$) [25-27], sphene ($CaTiSiO_5$) [28] or baghdadite ($Ca_3ZrSi_2O_9$) [29, 30] will form. Our previous study [31] had proved that the high dissolution rate of CS can be

effectively slowed down by the surface modification with nano-zinc silicate, and there was no phase change occurred in the original CS substrate. Nevertheless, CS bioceramic modified with pure nano-zinc silicate (Zn-CS) failed to release zinc ions (Zn^{2+}) because of its stable surface structure, moreover, only a few mineralized HA crystals could deposit on the surface of Zn-CS, which is disadvantageous to bone bonding.

Zinc (Zn) plays dual functional roles in bone tissue metabolism, it can not only help to promote bone formation through increasing the activity of osteoblast, but also simultaneously suppress bone resorption via decreasing the activity of osteoclast [32-35]. Dietary Zn supplementation is capable of down-regulating the expression of the tartrate resistant acid phosphatase (TRAP), which is associated with the osteoclast activity and bone resorption [36]. Furthermore, Zn can make osteoclast apoptosis via inhibiting its related gene expressions [33]. 10^{-6}–10^{-4} M of Zn was able to induce mouse osteoblast-like cells (MC3T3-E1) to up-regulate the expressions of runt-related transcription factor 2 (Runx-2), osteoprotegerin (OPG) and osteocalcin (OC) [37]. Therefore, it is necessary to improve the surface solubility of Zn-CS.

As a natural polysaccharide, sodium alginate (SA) has been widely used for the pharmaceutical and food applications [38], and SA is also convenient to be applied in film formation. As reported, zinc silicate nanoparticles with weak crystallinity possess good biocompatibility and biodegradable, and furthermore, zinc silicate is conducive to osteogenesis without cytotoxicity [39, 40]. In this study, sodium alginate/nano-zinc silicate (SA/nano-ZS) suspension was spin-coated on the surface of CS bioceramic disk, and a (Zn,Na)-containing silicate surface layer would form on its surface. We hope (Zn,Na)-

containing silicate surface layer not only could effectively control the dissolution rate of the CS substrates, but also released a certain amount of Zn. In vitro mineralization behavior as well as biological performance of SA/nano-ZS co-modified CS (Na/Zn-CS) was studied in detail, and a pure CS group was served as control. Rat bone marrow mesenchymal stem cells (rBMSCs) were used to assess the osteogenic performance of Na/Zn-CS.

2. Materials and Method

2.1. Materials

CS precursor powder was prepared via the chemical precipitation method as described in our previous study [31]. Briefly, 0.1 M sodium metasilicate nonahydrate ($Na_2SiO_3 \cdot 9H_2O$) solution was slowly added into 0.1 M calcium chloride ($CaCl_2$) solution with a constant stirring. Subsequently, CS precursor powder was collected by centrifugation and washed with deionized water for 3 times, and finally, the powder was oven-dried at 80^{o}C for 24 hours. Nano-zinc silicate powder was synthesized at 110 ^{o}C for 40 min by the microwave-assisted hydrothermal method using a microwave accelerated reaction system (Mars-5, CEM, USA) [40]. Zinc nitrate hexahydrate ($Zn(NO_3)_2 \cdot 6H_2O$) and tetraethyl orthosilicate (TEOS) were used as Zn source and Si source, respectively, and ammonia solution (25 wt.%) was added to accelerate the hydrolysis of TEOS. All the reagents used for synthesis were analytical pure and purchased from Sinopharm Chemical Reagent Co., Ltd in China.

CS precursor powder was filled in a cylindrical steel mould and pre-pressed at 30 MPa to form the CS precursor disks, then they were vacuum-packaged and transferred into a cold isostatic pressing equipment (LDJ100/320-300, Sichuan Chuanxi Machinery Co., Ltd, China), and isostatically pressed at 200 MPa to obtain the CS green disks. Hereafter, the obtained CS

green disks were sintered at 1150°C for 2 h in a furnace (HT16/17, Nabertherm, Germany) to get the densified CS bioceramic disks (Φ14×2 mm). Different concentrations of SA/nano-ZS suspensions were prepared by adding different amounts of nano-zinc silicate powders into the sodium alginate (B.R., Sigma-Aldrich, USA) solutions (3 wt.%), as shown in Table 1. Finally, SA/nano-ZS suspensions were spin-coated on the surface of the sintered CS disks, and sintered again at 1100°C for 2 h to obtain the Na/Zn-CS disks. Furthermore, the definitions of the abbreviations such as Na/0.1Zn-CS, Na/0.05Zn-CS, and Na/0.025Zn-CS were listed in Table 2. In addition, all CS and Na/Zn-CS disks were sterilized using the γ-ray irradiation (20kGy) before the biological assessments.

2.2. In vitro mineralization behavior

The in vitro mineralization experiments were carried out by soaking CS and Na/Zn-CS disks in simulated body fluid (SBF) for 4 weeks, respectively, and SBF was replenished once per week. SBF with similar ion concentrations to those in human blood plasma was prepared according to the method described by Kokubo and Takadama [41]. Briefly, reagent-grade components listed in Table 3 (Sinopharm Chemical Reagent Co., Ltd in China) were mixed together in distilled water to yield a final 2L solution containing 142.0 mM Na^+, 5.0 mM K^+, 1.5 mM Mg^{2+}, 2.5 mM Ca^{2+}, 103.0 mM Cl^-, 27.0 mM HCO^{3-}, 1.0 mM HPO_4^{2-}, 0.5 mM SO_4^{2-} at pH=7.4. CS disks and Na/Zn-CS disks were soaked in SBF with a surface area to volume ratio of 0.1 cm^2/mL, and they were continuously shaken in a shaking bath (770R, Aplus, USA) at 37°C with a speed of 60 rpm.

2.3. pH value of the soaking liquid

The SBF solutions in which CS disks and Na/Zn-CS disks had soaked were collected at

the predetermined intervals, respectively. Subsequently, the pH value of the collected SBF solutions was measured by using a pH meter (Sartorius, Germany). Each group has three parallel samples in this study.

2.4. Surface phase composition and morphology

After being soaked in SBF for 0, 1, 2, 3 weeks, the surface phases of CS disks and Na/Zn-CS disks were tested by X-ray diffractometer (XRD, X'Pert PRO, PANalytical, the Netherland) using a Cu*K*α source (λ=1.541874 Å), and the final components were ascertained by comparing their diffraction patterns with the Joint Committee on Powder Diffraction Standards (JCPDS) cards, respectively. In addition, the surface morphology of CS disks and Na/Zn-CS disks after being soaked in SBF for 0, 1, 2, 3 weeks was observed by using a field-emission scanning electron microscope (FE-SEM, Nova NanoSEM 430, FEI, USA) equipped with an energy dispersive X-ray spectrometer (EDS, INCA X-act, Oxford, U.K.), operated at an acceleration voltage of 10 kV. Furthermore, all CS and Na/Zn-CS disks were sputtered twice with gold before FE-SEM observing.

2.5. Cell cultures

The primary rBMSCs (Cat.No.CRL-12424) purchased from ATCC were maintained in cell culture flasks, and then they were subcultivated in a cell incubator at 37°C with a 5% CO_2 humidified atmosphere. As rBMSCs were almost confluent in the bottom of the cell culture flask, 0.25% trypsin/EDTA was added to make them detachment. Finally, they were collected and stored in a liquid nitrogen container for use. The rBMSCs after 4 times of passages were used in our following cell experiments. High-glucose Dulbecco's Modified Eagle's Medium (H-DMEM, Gibco, Cat.No.11965-092) with 10 vol.% fetal bovine serum (FBS, Hyclone,

Cat.No.NWJ0473) was applied for culturing rBMSCs, and the culture medium was refreshed every two days.

2.6. Cell viability assessment

The sterilized CS disk and Na/Zn-CS disk were transferred into 12-well culture plates, and serum-free H-DMEM medium was added to prewet them for 2 h before rBMSCs were seeded on their surface. The definitions of the abbreviations such as rBMSCs-CS and rBMSCs-Na/Zn-CS were listed in Table 2. 2 mL H-DMEM medium with 10% FBS was added into each well with a cell density of 1.2×10^5 cells/well, subsequently, the culture plates containing rBMSCs-Na/Zn-CS and rBMSCs-CS were set in a cell incubator (37°C with a 5% CO_2 humidified atmosphere) for 1, 3, 7 days. Moreover, culture medium was refreshed every two days. After being cultured for 1 day, rBMSCs-CS and rBMSCs-Na/Zn-CS were rinsed twice with phosphate buffer solution (PBS) and stained with Viability Assay Kit for Animal Live Cells (Calcein-AM, Biotium, USA) according to the instruction of the manufacturer. The fluorescent images of rBMSCs were acquired using a fluorescence microscope equipped with a digital camera (40FL Axioskop, Zeiss, Germany).

Quantitative cell viability assessment was measured by using a Cell Counting Kit-8 (CCK-8, Dojindo, Japan) assay. At the pre-determined intervals, rBMSCs-Na/Zn-CS and rBMSCs-CS were transferred into new 12-well plates, and then 600 μL CCK-8 working solution was added into each well to ensure all rBMSCs-CS and rBMSCs-Na/Zn-CS to be submerged. Subsequently, the plates were set in a cell incubator for 1 h. After the above incubation, 100 μL supernatant was extracted from each well and transferred into a new 96-well plate, and the absorbance of the supernatant was read at 405 nm using an enzyme linked

immunoadsorbent assay plate reader (Varioskan Flash, Thermo Scientific, USA).

2.7. Cell attachment, morphology and cytoskeletal organization

The rBMSCs were directly seeded on the surface of CS and Na/Zn-CS disks in a 12-well plate with a density of 1.2×10^5 cells/well. After incubation for 24 h, rBMSCs-CS and rBMSCs-Na/Zn-CS were rinsed with PBS twice, and then they were soaked in 2.5 vol.% glutaraldehyde solution for 4 h to immobilize the rBMSCs. In the following, rBMSCs-CS and rBMSCs-Na/Zn-CS were dehydrated with a graded series of ethanol (30 vol.%, 50 vol.%, 70 vol.%, 80 vol.%, 90 vol.%, 95 vol.% and 100 vol.%), and finally dried at room temperature. The attachment and morphology of rBMSCs seeded on the surface of CS and Na/Zn-CS disks were observed by SEM (Quanta 200, FEI, USA).

After rBMSCs were incubated on the surface of CS and Na/Zn-CS disks for 7 days, respectively, rBMSCs-CS and rBMSCs-Na/Zn-CS were rinsed with PBS once, and then soaked in 4 vol.% formaldehyde solution for 20 min to immobilize rBMSCs. Afterward rBMSCs-CS and rBMSCs-Na/Zn-CS were submerged in Triton X-100 solution (0.1 vol.%) for 5 min. The cytoskeletal organization of rBMSCs, cultured on the surface of the sample and on the plate margin around the sample in the same well, was investigated by labeling F-actin in fixed cells with green fluorescence using cell navigator™ F-actin labeling kit (AAT Bioquest, USA), which was strictly performed according to the kit protocol. To visualize the nucleus, rBMSCs were counterstained with DAPI staining solution (Beyotime, China). Fluorescence images of rBMSCs were obtained by using an inverted fluorescence microscope (Eclipsc Ti-U, Nikon, Japan).

2.8. Alkaline phosphatase (ALP) activity assay

rBMSCs were seeded on the surface of CS disks and Na/Zn-CS disks with a density of 3×10^5 cells/well, respectively. The rBMSCs-CS and rBMSCs-Na/Zn-CS were incubated in 12-well plate and 2 mL osteogenic induction culture medium was added to each well for culturing rBMSCs. H-DMEM containing 10 vol.% FBS, 10 mM sodium β-glycerophosphate, 0.1 μM dexamethasone and 50 mg/mL vitamin C were used as the osteogenic induction culture medium, and it was refreshed every other day. The ALP activity assay was performed after rBMSCs were cultured on the surface of CS disks and Na/Zn-CS disks for 7 and 14 days, respectively. At the predetermined intervals, rBMSCs-CS and rBMSCs-Na/Zn-CS were transferred into a new 12-well plate, and then gently rinsed by cold PBS for three times. 10 mM Tris-HCl solution (pH=7.4), 0.5 mM magnesium chloride solution ($MgCl_2$), 0.1 vol.% Triton X-100 solution were used for the preparation of lysis buffer. Subsequently, 600 μL lysis buffer was added to each sample for cell lysis at 4°C for 2 h. Afterward cells were sonicated for 20 s and centrifuged at 3000 rpm for 5 min at 4°C. Then 20 μL of the lysate was added to 200 μL of 5 mM p-nitrophenyl phosphate (p-NPP, Sigma-Aldrich) and incubated for 15 min at 37°C with the treatment of light avoidance. The reaction was stopped using 1 mL of 0.1 M NaOH and the absorbance was read at 405 nm by using an enzyme linked immunoadsorbent assay plate reader (Varioskan Flash, Thermo Scientific, USA). The ALP activity was calculated from a standard curve after normalizing to the total protein content, which was measured using Pierce BCA Protein Assay Kit (Thermo Scientific, USA). The results were expressed in millimoles of p-NPP produced per minute per milligram of protein.

2.9. Test of the released zinc ions (Zn^{2+})

As the culture medium was refreshed at the pre-determined intervals, the supernatants of

the replaced culture media were collected, respectively. Thereafter, the collected culture medium was digested by boiling it with concentrated nitric acid, and then the well digested culture medium was tested by an inductively coupled plasma atomic emission spectroscope (ICP-AES, Optima 5300DV, Perkin Elmer, USA) to obtain the concentration of Zn^{2+} released from Na/Zn-CS disks during the cell culture process.

2.10. Statistical Analysis

Quantitative data were presented as mean ± standard deviation, and statistical analyses were performed using a one-way analysis of variance (one-way ANOVA). A comparison between the two means was made using the turkey's test, with statistical significance set at $P < 0.05$.

3. Results

3.1. Surface phase composition of CS disks and Na/Zn-CS disks

All the diffraction peaks of CS disks (Fig. 1(a)) were in good agreement with those of anorthic pseudowollastonite phase calcium silicate (JCPDS card no. 074-0874). However, obvious phase change could be found after the surface modification of CS disks with different concentrations of SA/nano-ZS suspensions. As shown in Fig. 1(b), the surface composition of Na/0.025Zn-CS disks was composed of Na/Ca co-doped zinc silicate (Shibkovite, JCPDS card no. 051-1432), sodium calcium silicate ($Na_4Ca_4Si_6O_{18}$, JCPDS card no. 01-079-1089) and pseudowollastonite phase calcium silicate. Moreover, Na/0.05Zn-CS disks (Fig. 1(c)) and Na/0.1Zn-CS (Fig. 1(d)) disks had the same surface composition as Na/0.025Zn-CS disks.

3.2. Mineralization performance of Na/Zn-CS disks after being soaked in SBF

After being soaked in SBF for 1 week, it was found in Fig. 2(a) that Na/Zn co-doped HA

(JCPDS card no. 01-070-3371) as well as sodium zinc phosphate hydrate ($NaZn(PO_4)\cdot H_2O$, JCPDS card no. 01-089-6669) could deposit on the surface of Na/0.1Zn-CS disks. As the soaking time increased, pseudowollastonite phase calcium silicate, sodium calcium silicate and Na/Ca co-doped zinc silicate were continuously dissolving. When the soaking time prolonged to 3 weeks, in spite of a small amount of pseudowollastonite phase calcium silicate and sodium calcium silicate, the surface of Na/0.1Zn-CS disk was almost covered by Na/Zn co-doped HA. Similar to Na/0.1Zn-CS disks, the primary Na/Ca co-doped zinc silicate, sodium calcium silicate and pseudowollastonite phase calcium silicate progressively dissolved with the prolongation of the soaking time, and Na/Zn co-doped HA finally deposited on the surface of Na/0.05Zn-CS disks (Fig. 2(b)), but sodium zinc phosphate hydrate could not be found until Na/0.05Zn-CS disks were soaked in SBF for 2 weeks. Its surface was almost covered by Na/Zn co-doped HA after Na/0.025Zn-CS disk was soaked in SBF for 2 weeks, but no sodium zinc phosphate hydrate could be found on its surface, as shown in Fig. 2(c).

After Na/0.025Zn-CS disks were soaked in SBF for 1 week, the pH value of the collected SBF, raised from 7.4 to 7.7, whereas it would rapidly declined from the second week, and fluctuated at a narrow range with the increase of soaking time, as illustrated in Fig. 3. Na/0.1Zn-CS disks and Na/0.05Zn-CS disks had the similar variation trend as that of Na/0.025Zn-CS disks. Nevertheless, the pH value of the collected SBF, in which CS disks had been soaked, continued to increase with the prolongation of the soaking time. Fig. 4A displays the surface morphology of Na/0.1Zn-CS disk after being soaked in SBF for 1 week, and its partial surface area was covered by Zn/Na co-doped HA (the regions where white arrows directed in Fig. 4A). The (Zn,Na)-containing surface layer (the regions where black arrows

directed in Fig. 4B) of Na/0.1Zn-CS disk gradually dissolved, and Zn/Na co-doped HA deposited on the surface of the CS substrate (the regions where white arrows directed in Fig. 4B). In the same conditions, many pores with a size ranging in 10–100 μm formed on the surface of Na/0.05Zn-CS disk (Fig. 4C), but most of the surface of Na/0.025Zn-CS disk was covered by Zn/Na co-doped HA (Fig. 4D). As the soaking time prolonged to 2 weeks, more Zn/Na co-doped HA deposited on the surface of Na/0.1Zn-CS disk (Fig. 4E). Owing to its surface dissolution, some big pores formed on the surface of Na/0.1Zn-CS disk. In addition, small Zn/Na co-doped HA crystals also could be found depositing on the wall of the pores, which spread along the wall of the pores like creepers (Fig. 4F). If all other conditions were equal, a relative dense mineralized Zn/Na co-doped HA layer was formed on the surfaces of Na/0.05Zn-CS disks and Na/0.025Zn-CS disks after they were soaked in SBF for 2 weeks, respectively, which were shown in Figs. 4G-4H.

3.3. Viability and proliferation of rBMSCs cultured on the surfaces of CS disks and Na/Zn-CS disks

In Fig. 5, only a small amount of viable rBMSCs (green fluorescence) could be found on the surface of Na/0.025Zn-CS disks and Na/0.05Zn-CS disks, and some rBMSCs seemed to sink in the pores. Nevertheless, more viable rBMSCs attached on the surfaces of Na/0.1Zn-CS disks and CS disks. After being cultured on the surface of CS disks, Na/0.025Zn-CS disks, Na/0.05Zn-CS disks and Na/0.1Zn-CS disks for 7 days, respectively, rBMSCs significantly proliferated (Fig. 6), which suggests the above bioceramics have good biocompatibility. However, comparing to that of Na/0.025Zn-CS disks and Na/0.05Zn-CS disks, the rBMSCs cultured on the surface of CS disks for 7 days had a better proliferation. It is well accepted

that OD value is proportional to the quantity of viable rBMSCs. From the first day to the third day, the increased OD value of Na/0.025Zn-CS disks, Na/0.05Zn-CS disks, Na/0.1Zn-CS disks and CS disks was 0.0946, 0.0326, 0.059 and 0.238, respectively, indicating that the rBMSCs cultured on the surface of CS disks proliferated more quickly in this period. But from the third day to the seventh day, the increased OD value of Na/0.025Zn-CS disks, Na/0.05Zn-CS disks, Na/0.1Zn-CS disks and CS disks was 0.5134, 0.1238, 0.8161 and 0.6374, respectively, which indicated the rBMSCs seeded on the surface of Na/0.1Zn-CS disks had a faster proliferation in the last four days by comparing with those cultured on the surface of CS disks.

3.4. Attachment, spread and cytoskeletal organization of rBMSCs after being cultured on the surfaces of CS disks and Na/Zn-CS disks

As displayed in Fig. 7, rBMSCs possessed an ellipsoidal shape with a size of 10–15 μm, and they had several filopodia. Whether rBMSCs were cultured on the surface of CS disk or Na/Zn-CS disk, they did not attach and spread well on its surface. The rBMSCs cultured on the surface of Na/0.05Zn-CS disks seemed to hang in the sky and supported its own weight only by using several filopodia to adhere to the walls of the pore (Fig. 7C). The rBMSCs surface (Fig. 7D) was covered by many tiny particles, similar to the mineralized HA crystals which deposited on the surface of CS disks and Na/Zn-CS disks. Furthermore, EDS testing result (Fig. 7E) indicated that the surface composition of rBMSCs consisted of Ca and P elements (detected on the surface of rBMSCs in the Fig. 7D where the red * directed), which further confirmed the mineralization occurred on the surfaces of rBMSCs.

In order to demonstrate the presence of actin filaments in rBMSCs, which were cultured

on the surface of Na/Zn-CS disks and CS disks, cytoskeletal organization was determined by staining rBMSCs with iFluor^{TM}488-phalloidin. After seeded on the surface of CS disks and Na/0.1Zn-CS disks for 7 days, rBMSCs did not spread well (Fig. 8), only faint and poorly organized actin stress fibers were found in rBMSCs. Moreover, the actin stress fiber produced by rBMSCs was also less, and no cytoplasmic meshwork could be observed in rBMSCs. However, rBMSCs spread well on the plate margin around the bioceramic disk when all other conditions were equal, and they also produced more distinct and well defined stress fibers as well as actin-containing microfilaments (Fig. 9). Different from the rBMSCs attached on the surface of bioceramic disk (Fig. 8), the rBMSCs with a cytoplasmic meshwork were observed on the plate (red arrows directed region in Fig. 9), and their cytoskeleton obviously expanded.

3.5. Differentiation of rBMSCs cultured on the surfaces of CS disks and Na/0.1Zn-CS disks

Cell differentiation ability is closely related with the ALP activity. As shown in Fig. 10, after incubation for 7 days, no significant differences could be found, and the ALP activity of rBMSCs cultured on the surface of CS disks was very close to that cultured on the surface of Na/0.1Zn-CS disks. When culture time prolonged to 14 days, the ALP activity of rBMSCs cultured on the surface of both bioceramic disks increased, but the ALP activity of rBMSCs cultured on the surface of Na/0.1Zn-CS disks was significantly higher than that cultured on the surface of CS disks. In addition, ICP testing results proved that Zn^{2+} could be dissolved out from Na/0.1Zn-CS disks during the cell culture process (Table 4).

4. Discussion

The ionic radius of Zn^{2+} (74 pm) is smaller than that of Ca^{2+} (100 pm). According to the Law of Coulomb, the bonding strength of Zn-O should be stronger than that of Ca-O.

Furthermore, different from Ca^{2+}, Zn^{2+} exhibit partial covalent interactions in tetrahedral environment [42]. The dissolution rate of "45S5" bioglass obviously decreased with the incorporation of Zn, and almost no apatites could deposit on its surface when 20 wt.% of Zn were incorporated into "45S5" bioglass [43]. Moreover, the degradation of Zn-containing silica-based bioglass became slower than that without Zn [44]. In addition, hardystonite also showed poor degradability, and Zn^{2+} was hard to be dissolved out [20]. In fact, our previous study also proved that the structural stability of CS could be improved by only using Zn atom to partially substitute for Ca atom [31]. The ionic radius of Na^{+} is similar (102 pm) to that of Ca^{2+}, but it has lower valence by comparing with Ca^{2+} or Zn^{2+}. For the sake of the coordination, more Na atoms have to substitute for Ca or Zn atoms, which will reduce the structural stability of Zn-containing surface layer, so it well explains why (Zn,Na)-containing surface layer had higher dissolution rate than that of Zn-containing surface layer.

Actually, Zn atom played a role in improving the structural stability of CS, whereas Na atom had negative effect on maintaining its structural stability. Therefore, the dissolution rate of (Zn,Na)-containing surface layer is ascribed to its molar ratio of Na/Zn. The result of EDS (listed in Table 5) indicated, the Na/Zn molar ratio on the surface of Na/0.025Zn-CS disk, Na/0.05Zn-CS disk and Na/0.1Zn-CS disk is 5.98, 4.39, 3.13, respectively. Therefore, Na/0.025Zn-CS disk had a (Zn,Na)-containing surface layer with relatively higher Na/Zn ratio, so its surface dissolved faster than that of Na/0.1Zn-CS disk, and the fast surface dissolution could lead to rapid deposition of Na/Zn co-doped HA on its surface (Fig. 4D), which benefits for its bonding to the bone tissue. However, the interface stability of the cell/material had significant influences on cell attachment, cell spreading and the initial cell

proliferation, and rBMSCs preferred attaching and spreading on a stable contact surface. The composition as well as topography of the hardystonite bioceramic could modulate the attachment and proliferation of human osteoblast-like cells (HOBs) [20]. But the inorganic ions (such as Zn^{2+}, Na^{+}) released from Na/Zn-CS disks had few effects on the attachment and spreading of rBMSCs, as proved by comparing Fig. 8 with Fig. 9. Zhang N.L. reported that the cell attachment and viability for fine-grained pseudowollastonite (psWf, roughness 0.74 μm) was lower than that for coarse-grained pseudowollastonite (psWc, roughness 1.25 μm) surface because of the faster surface dissolution of psWf [45]. Thus, a proper surface dissolution rate of biomaterials may be good for bone bonding and initial cell growth.

Bone mesenchymal stem cell has the ability to differentiate into osteoblast. During the process of bone formation, osteoblast is the primary functional cell which is responsible for the synthesis, secretion and mineralization of bone matrix. Therefore, rBMSCs were used for evaluating the osteoinductivity of CS disk and Na/Zn-CS disk in this study. The extracellular mineralization phenomenon was found on the surface of rBMSCs (Fig. 7), which suggested Si possessed osteoinductivity and rBMSCs had great possibilities to differentiate into the rat osteoblasts. Si released from the siloxane-doped poly(lactic acid)/vaterite composite scaffold could induce the formation of bone nodules on the surface of HOBs [46]. Furthermore, J. R. Jones [47] reported that the released Si was able to stimulate the synthesis of the bone matrix protein collagen I, which would induce the mineralization of HOBs. However, to the best of our knowledge, when cells are cultured with HA, β-TCP and CPC, no extracellular mineralization phenomenon can be observed. Recently, in order to enhance their osteoinductivity, more and more researchers tried to incorporate Si into calcium phosphate

based bone repair materials [48,49]. Nevertheless, the pathway and mechanism of Si to induce bone formation remains unclear up to now, and it will be further studied in the future.

As previously discussed, fast surface dissolution was detrimental to the initial cell growth, so rBMSCs cultured on the surface of Na/0.1Zn-CS disks proliferated slower than that cultured on the surface of CS disks in the first three days, as shown in Fig. 6. However, rBMSCs cultured on the surface of Na/0.1Zn-CS disks had higher proliferation rate in the last four days by comparing with that cultured on the surface of CS, which further proved the released Zn could indeed promote the proliferation of rBMSCs. Moreover, it was also found that the released Zn had the ability to stimulate rBMSCs to up-regulate the expression of ALP activity. Zn is a key element in ALP which is central to the mineralization of bone matrix [35]. Inhibiting the dissociation of the active Zn center can result in increasing the lifetime of the ALP molecule. Interestingly, Hall S. L. [50] found that the presence of Zn could increase ALP specific activity (at least in a human osteosarcoma cell line), and no similar effect was seen for a variety of other elements, including but not limited to Ca, Mg, Mn. Moreover, Zn in TCP helped to enhance the ALP activity of human bone marrow stromal cells (hBMSCs). Calcium phosphate cement implants with 0.03 wt.% Zn can significantly promote the formation of new bone [51]. MC3T3-E1 and mesenchymal stem cells (MSCs) cultured on the Zn-HA layer showed better ALP activity and up-regulated gene expression of osteocalcin in comparison with that cultured on the HA layer [52,53]. Wang X. P. [54] reported that Zn released from a Zn-containing bioglass scaffold promoted the ALP activity of MSCs.

5. Conclusion

Sodium alginate/nano-zinc silicate co-modified calcium silicate (Na/Zn-CS) bioceramic

disks were successfully prepared via the spin-coating process. By comparing with pure pseudowollastonite phase calcium silicate (CS) bioceramic disks, Na/Zn-CS bioceramic disks not only had a proper dissolution rate, but also could induce HA to deposit rapidly on their surfaces. Whether rBMSCs were cultured on the surface of CS disk or Na/Zn-CS disk, the extracellular matrix mineralization could be observed on the surface of rBMSCs, which suggests Si probably possesses osteoinductivity. In addition, the interface stability of the cell/material had great influences on the cell attachment, cell spreading and the initial cell proliferation. In this study, rBMSCs preferred attaching and spreading on a stable surface. Owing to the released Zn, the proliferation and differentiation of rBMSCs cultured on the surface of CS disk spin-coated with 0.1 g/mL of SA/nano-ZS suspension were significantly promoted. In summary, Na/Zn-CS bioceramic has great potentials for the application of bone regeneration.

Acknowledgments

This work is financially supported by the National Basic Research Program of China (Grant No. 2012CB619100) and the National Natural Science Foundation of China (Grant No. 51402247, 51172074). Thanks Dr. Jing Zhang for her effort work in evaluating the cell-biological performances of CS disk and Na/Zn-CS disk.

References

[1] Ni S, Chang J, Chou L. A novel bioactive porous $CaSiO_3$ scaffold for bone tissue engineering. J Biomed Mater Res A 2006;76(1):196-205.

[2] Sarmento C, Luklinska ZB, Brown L, Anseau M, De Aza PN, De Aza S, et al. In vitro behavior of osteoblastic cells cultured in the presence of pseudowollastonite ceramic. J Biomed Mater Res A 2004;69A(2):351-8.

[3] Zuleta F, Velasquez PA, De Aza PN. In vitro characterization of laser ablation pseudowollastonite coating. Mater Sci Eng C-Mater 2011;31(2):377-83.

[4] Raquez JM, Barone DTJ, Luklinska Z, Persenaire O, Belayew A, Eyckmans J, Schrooten J, Dubois P. Osteoconductive and Bioresorbable Composites Based on Poly(L,L-lactide) and Pseudowollastonite: From Synthesis and Interfacial Compatibilization to In Vitro Bioactivity and In Vivo Osseointegration Studies. Biomacromolecules 2011;12(3):692-700.

[5] Xue WC, Liu XY, Zheng XB, Ding CX. In vivo evaluation of plasma-sprayed wollastonite coating. Biomaterials 2005;26(17):3455-60.

[6] Wei J, Chen FP, Shin JW, Hong H, Dai CL, Su JC, Liu CS. Preparation and characterization of bioactive mesoporous wollastonite-Polycaprolactone composite scaffold. Biomaterials 2009;30(6):1080-8.

[7] Dou YD, Wu CT, Chang J. Preparation, mechanical property and cytocompatibility of poly(L-lactic acid)/calcium silicate nanocomposites with controllable distribution of calcium silicate nanowires. Acta Biomater 2012;8(11):4139-50.

[8] Wu CT, Fan W, Zhou YH, Luo YX, Gelinsky M, Chang J, Xiao Y. 3D-printing of highly uniform $CaSiO_3$ ceramic scaffolds: preparation, characterization and in vivo osteogenesis. J Mater Chem 2012;22(24):12288-95.

[9] Ni SY, Chang J, Chou L, Zhai WY. Comparison of osteoblast-like cell responses to calcium silicate and tricalcium phosphate ceramics in vitro. J Biomed Mater Res B: Appl Biomater 2007;80B:174-183.

[10] Mertz W. The essential trace elements. Science 1981;213:1332-8.

[11] Carlisle E.M. Silicon: a requirement in bone formation independent of vitamin D1 [J]. Calcif Tissue Int 1981, 33(1):27-34.

[12] Carlisle E.M. Silicon, A possible factor in bone calcification [J]. Science 1970, 167:279-280.

[13] EI-Ghannam A, Ducheyne P, Shapiro IM. Formation of surface reaction products on bioactive glass and their effects on the expression of the osteoblastic phenotype and the deposition of mineralized extracellular matrix. Biomaterials 1997;18(4):295-303.

[14] Au AY, Au RY, Demko JL, McLaughlin RM, Eves BE, Frondoza CG. Consil bioactive glass particles enhance osteoblast proliferation and selectively modulate cell signaling pathways in vitro. J Biomed Mater Res A 2010;94(2):380-388.

[15] Casey WH, Westrich HR, Banfield JF, Ferruzzi G, Arnold GW. Leaching and Reconstruction at the Surface of Dissolving Chain-Silicate Minerals. Nature 1993;366:253-6.

[16] Sung-Back C, Nakanishi K, Kokubo T, Soga N, Ohtsuki C, Nakamura T, Kitsugi T, Yamaguro T. Dependence of Apatite Formation on Silica Gel on Its Structure: Effect of Heat Treatment. J Am Ceram Soc 1995;78(7)1769-74.

[17] Zhai WY, Lu HX, Chen L, Lin XT, Huang Y, Dai KR, Naoki K, Chen GP, Chang J. Silicate bioceramics induce angiogenesis during bone regeneration. Acta Biomater 2012;8(1):341-9.

[18] Li HY, Chang J. Stimulation of proangiogenesis by calcium silicate bioactive ceramic. Acta Biomater 2013;9(2):5379-89.

[19] Wang C, Lin KL, Chang J, Sun J. Osteogenesis and angiogenesis induced by porous β-

$CaSiO_3$/PDLGA composite scaffold via activation of AMPK/ERK1/2 and P13K/Akt pathways. Biomaterials 2013;34(1):64-77.

[20] Ramaswamy Y, Wu CT, Zhou H, Zreiqat H. Biological response of human bone cells to zinc-modified Ca-Si-based ceramics. Acta Biomater 2008;4(5):1487-97.

[21] Zreiqat H, Ramaswamy Y, Wu CT, Paschalidis A, Lu ZF, James B, Brike O, McDonald M, Litte D, Dunstan CR. The incorporation of strontium and zinc into a calcium-silicon ceramic for bone tissue engineering. Biomaterials 2010;31(12):3175-84.

[22] Huang Y, Jin XG, Zhang XL, Sun HL, Tu JW, Tang TT, Chang J, Dai KR. In vitro and in vivo evaluation of akermanite bioceramics for bone regeneration. Biomaterials 2009;30(28):5041-48.

[23] Sun HL, Wu CT, Dai KR, Chang J, Tang TT. Proliferation and osteoblastic differentiation of human bone marrow-derived stromal cells on akermanite-bioactive ceramics. Biomaterials 2006;27(33):5651-7.

[24] Gu HJ, Guo FF, Zhou X, Gong LL, Zhang Y, Zhai WY, Chen L, Cen L, Yin S, Chang J, Cui L. The Stimulation of Osteogenic Differentiation of Human Adipose-Derived Stem Cells by Ionic Products from Akermanite Dissolution via Activation of the ERK Pathway. Biomaterials 2011;32(29):7023-33.

[25] Sainz MA, Pena P, Serena S, Caballero A. Influence of design on bioactivity of novel $CaSiO_3$-$CaMg(SiO_3)_2$ bioceramics: In vitro simulated body fluid test and thermodynamic simulation. Acta Biomater 2010;6(7):2797-2807.

[26] Wu CT, Ramaswamy Y, Zreiqat H. Porous diopside ($CaMgSi_2O_6$) scaffold: A promising bioactive material for bone tissue engineerings. Acta Biomater 2010;6(6):2237-45.

[27] Wu CT, Zreiqat H. Porous bioactive diopside ($CaMgSi_2O_6$) ceramic microspheres for drug delivery. Acta Biomater 2010;6(3):820-9.

[28] Ramaswamy Y, Wu CT, Ramaswamy Y, Dunstan CR, Hewson B, Eindorf T, Anderson GI, Zreiqat H. Sphene ceramics for orthopedic coating applications: An in vitro and in vivo study. Acta Biomater 2009;5(8):3192-3204.

[29] Roohani-Esfahani SI, Dunstan CR, Davies B, Pearce S, Williams R, Zreiqat H. Repairing a critical-sized bone defect with highly porous modified and unmodified baghdadite scaffolds. Acta Biomater 2012;8(11):4162-4172.

[30] Liang Y, Xie YT, Ji H, Huang LP, Zheng XB. Excellent Stability of Plasma-Sprayed Bioactive $Ca_3ZrSi_2O_9$ Ceramic Coating on Ti-6Al-4V. Appl Surf Sci 2010;256(14):4677-81.

[31] Xiong K, Shi HS, Liu JQ, Shen ZH, Li HY, Ye JD. Control of the Dissolution of Ca and Si Ions from $CaSiO_3$ Bioceramic via Tailoring Its Surface Structure and Chemical Composition. J Am Ceram Soc 2013;96(3):691-6.

[32] Yamaguchi M, Weitzmann MN. Zinc stimulates osteoblastogenesis and suppresses osteoclastogenesis by antagonizing NF-kappa B activation. Mol Cell Biochem 2011;355(1-2):179-86.

[33] Moonga BS, Dempster DW. Zinc is a potent inhibitor of osteoclastic bone resorption in vitro. J Bone Miner Res 1995;10(3):453-457.

[34] Lakhkar NJ, Lee IH, Kim HW, Salih V, Wall IB, Knowles JC. Bone formation controlled by biologically relevant inorganic ions: Role and controlled delivery from phosphate-based glasses. Adv Drug Deliver Rev 2013; 65(4):405-20.

[35] Habibovic P, Barralet JE. Bioinorganics and biomaterials: Bone repair. Acta Biomater 2011;7(8):3013-26.

[36] Dimai HP, Hall SL, Stilt-Coffing B, Farley JR. Skeletal response to dietary zinc in adult female mice. Calcif Tissue Int 1998;62(4):309-15.

[37] Yamaguchi M, Goto M, Uchiyama S, Nakagawa T. Effect of zinc on gene expression in osteoblastic MC3T3-E1 cells: enhancement of Runx2, OPG, and regucalcin mRNA expressions. Mol Cell Biochem 2008;312(1-2):157-66.

[38] Lee KY, Mooney DJ. Alginate: Properties and biomedical applications. Prog Polym Sci 2012;37(1):106-26.

[39] Zhang ML, Zhai WY, Chang J. Preparation and characterization of a novel willemite bioceramic. J Mater Sci-Mater Med 2010; 21(4):1169-73.

[40] Xiong K, Liu JQ, Li JY, Ye JD. Microwave-assisted hydrothermal synthesis of submicrometer willemite phase zinc silicate and its zinc ion release behavior. J Am Ceram Soc 2013;96(2):657-664.

[41] Kokubo T, Takadama H. How useful is SBF in predicting in vivo bone bioactivity. Biomaterials 2006;27(15):2907-2915.

[42] Jaroch DB, Clupper DC. Modulation of zinc release from bioactive sol-gel derived SiO_2-CaO-ZnO glasses and ceramics. J Biomed Mater Res A 2007;82A(3):575-88.

[43] Aina V, Malavasi G, Pla AF, Munaron L, Morterra C. Zinc-containing bioactive glasses: Surface reactivity and behaviour towards endothelial cells. Acta Biomater 2009;5(4):1211-22.

[44] Courtheoux L, Lao J, Nedelec JM, Jallot E. Controlled bioactivity in zinc-doped sol-gel-

derived binary bioactive glasses. J Phys Chem C 2008;112(35):13663-7.

[45] Zhang NL, Molenda JA, Fournelle JH, Murphy WL, Sahai N. Effects of pseudowollastonite ($CaSiO_3$) bioceramic on *in vitro* activity of human mesenchymal stem cells. Biomaterials 2010;31(30):7653-65.

[46] Obata A, Kasuga T. Stimulation of human mesenchymal stem cells and osteoblasts activities in vitro on silicon-releasable scaffolds. J Biomed Mater Res A 2009;91A(1): 11-7.

[47] Jones JR, Tsigkou O, Coates EE, Stevens MM, Polak JM, Hench LL. Extracellular matrix formation and mineralization on a phosphate-free porous bioactive glass scaffold using primary human osteoblast (HOB) cells. Biomaterials 2007;28(9):1653-63.

[48] Tomoaia G, Mocanu A, Vida-Simiti I, Jumate N, Bobos LD, Soritau O, Tomoaia-Cotisel M. Silicon effect on the composition and structure of nanocalcium phosphates In vitro biocompatibility to human osteoblasts. Mat Sci Eng C-Mater 2014; 614:31-4.

[49] Fielding G, Bose S. SiO_2 and ZnO dopants in three-dimensionally printed tricalcium phosphate bone tissue engineering scaffolds enhance osteogenesis and angiogenesis in vivo. Acta Biomater 2013; 9(11):9137-48.

[50] Hall SL, Dimai HP, Farley JR. Effect of zinc on human skeletal alkaline phosphatase activity in vitro. Calcif Tissue Int 1999;64(2):163-72.

[51] Li X, Sogo Y, Ito A, Mutsuzaki H, Ochiai N, Kobayashi T, Nakamura S, Yamashita K, LeGeros RZ. The optimum zinc content in set calcium phosphate cement for promoting bone formation in vivo. Mat Sci Eng C-Bio S 2009;29(3):969-75.

[52] Yang F, Wen JD, He FM, Wang XX, Zhao SF, Yang GL. Osteoblast response to porous

titanium surfaces coated with zinc substituted hydroxyapatite. Oral Surg Oral Med O 2011;113(3):313-8.

[53] Wang XP, Ito A, Sogo Y, Li X, Oyane A. Zinc-containing apatite layers on external fixation rods promoting cell activity. Acta Biomater 2010;6(3):962-8.

[54] Wang XP, Li X, Ito A, Sogo Y. Synthesis and characterization of hierarchically macroporous and mesoporous CaO-MO-SiO_2-P_2O_5 (M = Mg, Zn, Sr) bioactive glass scaffolds. Acta Biomater 2011;7(10):3638-44.

Figure Caption:

Figure 1 XRD patterns of (a) pure CS disk, (b) Na/0.025Zn-CS disk, (c) Na/0.05Zn-CS disk, and (d) Na/0.1Zn-CS disk.

Figure 2 XRD patterns of the surface of (a) Na/0.1Zn-CS disk, (b) Na/0.05Zn-CS disk and Na/0.025Zn-CS disk after being soaked in the SBF solution for 0, 1, 2, 3 weeks, respectively.

Figure 3 The pH value of the SBF solution in which CS disks and Na/Zn-CS disks have been soaked. (SBF were replenished once per week, n=3)

Figure 4 SEM images of the surface morphology of (A, B) Na/0.1Zn-CS disk, (C) Na/0.05Zn-CS disk and (D) Na/0.025Zn-CS disk after being soaked in SBF for 1 week; SEM images of (E) the surface morphology of Na/0.1Zn-CS disk, (F) the wall of the pores in the surface of Na/0.1Zn-CS disk, the surface morphology of (G) Na/0.05Zn-CS disk and (H) Na/0.025Zn-CS disk after being soaked in the SBF solution for 2 weeks. The black arrows in B indicate the original (Zn, Na)-containing layer on the surface of Na/0.1Zn-CS disk, and the white arrows in A and B indicate the deposited Zn/Na co-doped HA layer after Na/0.1Zn-CS disk being soaked in SBF for 1 week.

Figure 5 The live cell staining fluorescence images of rBMSCs cultured on the surface of Na/Zn-CS disk and CS disk for 1 day, respectively.

Figure 6 The proliferation of rBMSCs cultured on the surface of Na/Zn-CS disk and CS disk for 1, 3, 7 days, respectively. (n=4) *The Na/Zn-CS group compared with the CS group, $P<0.05$. CS is used as the control group and 0.64% phenol solutions were used as the positive control (Ctr^{+}).

Figure 7 SEM images of rBMSCs attached on the surface of (A) CS disk, (B) Na/0.1Zn-CS disk, (C) Na/0.05Zn-CS disk and (D) Na/0.025Zn-CS disk after being co-cultured for 1 day. (E) EDS test result of the element composition of tiny particles (red *) deposited on the surface of rBMSCs.

Figure 8 The staining images of F-actin (green, left), nucleus (blue, middle) and their merged images (right) of rBMSCs cultured on the surface of CS disk and Na/0.1Zn-CS disk for 7 days, respectively.

Figure 9 The staining images of F-actin (green, left), nucleus (blue, middle) and their merged images (right) of rBMSCs attached on the 12-well plate when they were co-cultured with CS disks and Na/0.1Zn-CS disk for 3, 7 days, respectively. Red arrows directed region refers to the cytoplasmic meshwork, which was formed by the expanding of the cytoskeleton.

Figure 10 The ALP activities of rBMSCs cultured on the surface of CS disk and Na/0.1Zn-CS disk for 7, 14 days, respectively. (n=4) *The Na/0.1Zn-CS group compared with the pure CS group after the incubation for 14 days, $P<0.05$.

Tables

Table 1 The composition of the sodium alginate/nano-zinc silicate suspensions.

Sample	Nano-Zinc Silicate (g)	Sodium Alginate (g)	Deionized Water (mL)
Na/0.1Zn	0.4	0.1237	4
Na/0.05Zn	0.2	0.1237	4
Na/0.025Zn	0.1	0.1237	4

Table 2 The definitions of the abbreviations used in this study.

Abbreviation	Definition
SA/nano-ZS	Sodium alginate/nano-zinc silicate suspension
SA	Sodium alginate
CS	Pseudowollastonite phase calcium silicate
Zn-CS	Pure nano-zinc silicate modified CS
Na/Zn-CS	SA/nano-ZS co-modified CS
Na/0.1Zn-CS	SA/nano-ZS (0.1 g/mL) co-modified CS
Na/0.05Zn-CS	SA/nano-ZS (0.05 g/mL) co-modified CS
Na/0.025Zn-CS	SA/nano-ZS (0.025 g/mL) co-modified CS
rBMSCs-CS	the cell-bioceramic construct that rBMSCs were seeded on the surface of CS disks
rBMSCs-Na/Zn-CS	the cell-bioceramic construct that rBMSCs were seeded on the surface of Na/Zn-CS disks

Table 3 The amounts of each chemical regent in SBF (2L).

Order	Regent	Amount
1	NaCl	16.07 g
2	$NaHCO_3$	0.71 g
3	KCl	0.45 g
4	$K_2HPO_4 \cdot 3H_2O$	0.462 g
5	$MgCl_2 \cdot 6H_2O$	0.622 g
6	HCl (1M)	78 mL
7	$CaCl_2$	0.584 g
8	Na_2SO_4	0.144 g
9	Tris	12.236 g

Table 4 The contents of Zn^{2+} released from Na/0.1Zn-CS disks as co-cultured with rBMSCs.

Culture Time (day)	1	3	13	15
Zn（μM）	13.54	4.27	5.64	3.46

Table 5 The Na/Zn molar ratio on the surface of Na/Zn-CS disks which were surface co-modified with different concentrations of SA/nano-ZS suspensions.

Sample	Na (Atomic Conc %)	Zn (Atomic Conc %)	Molar ratio of Na/Zn
Na/0.025Zn-CS	2.75	0.46	5.98

Na/0.05Zn-CS	6.63	1.51	4.39
Na/0.1Zn-CS	9.23	2.95	3.13

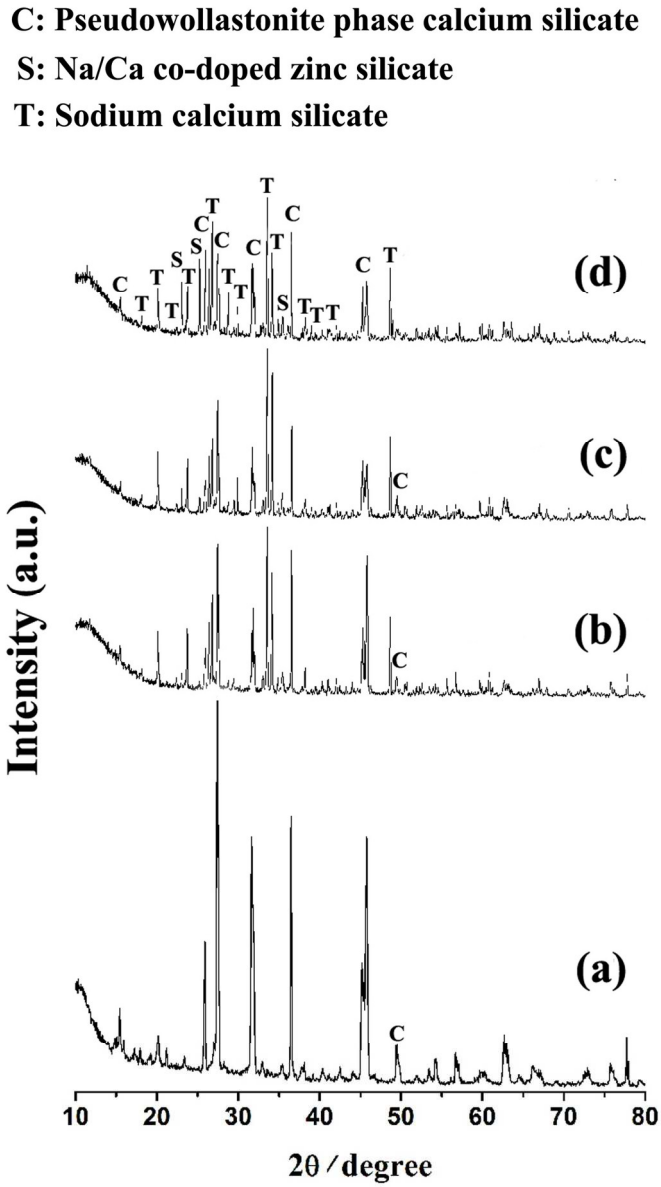

Figure 1 XRD patterns of (a) pure CS disk, (b) Na/0.025Zn-CS disk, (c) Na/0.05Zn-CS disk, and (d) Na/0.1Zn-CS disk.
114x200mm (300 x 300 DPI)

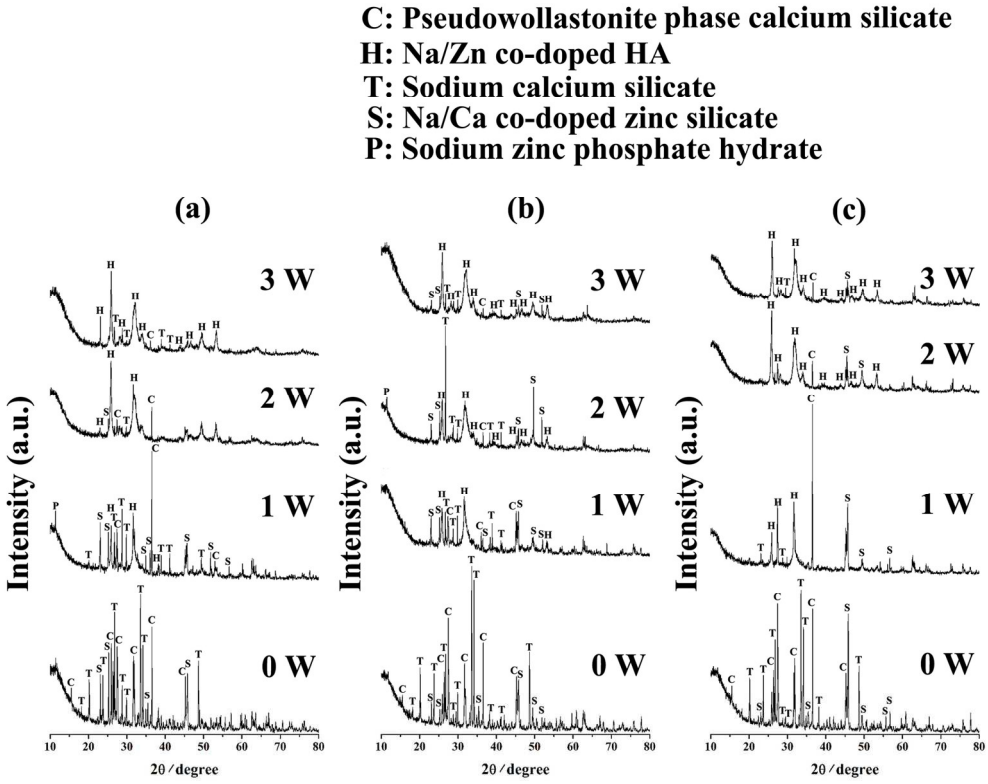

Figure 2 XRD patterns of the surface of (a) Na/0.1Zn-CS disk, (b) Na/0.05Zn-CS disk and Na/0.025Zn-CS disk after being soaked in the SBF solution for 0, 1, 2, 3 weeks, respectively.
160x127mm (300 x 300 DPI)

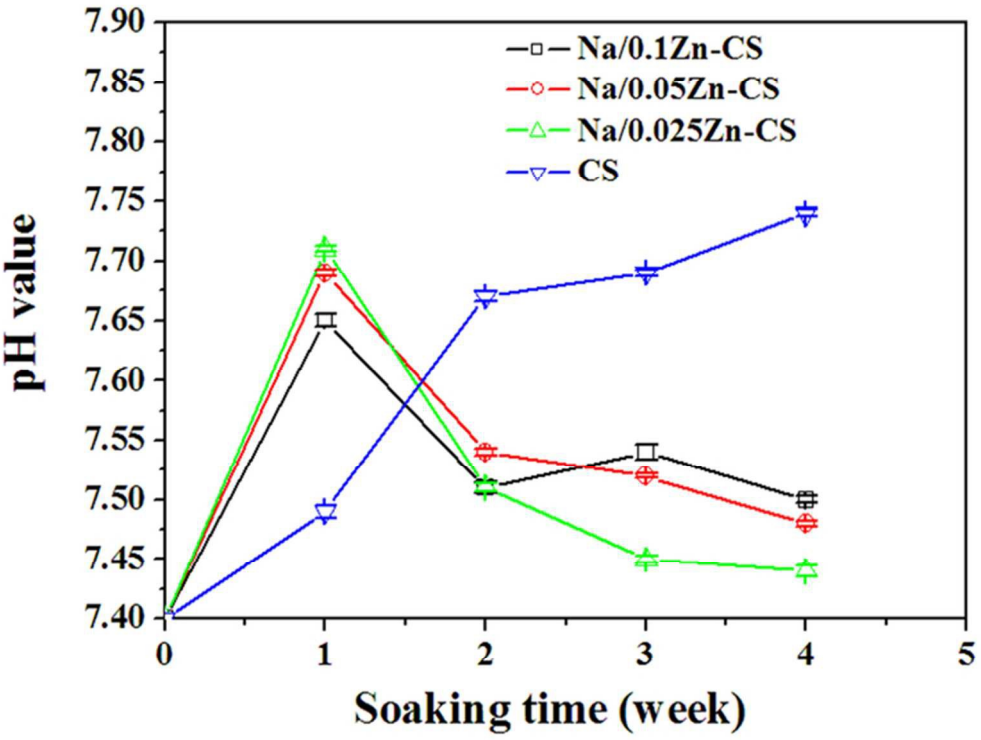

Figure 3 The pH value of the SBF solution in which CS disks and Na/Zn-CS disks have been soaked. (SBF were replenished once per week, n=3)
61x47mm (300 x 300 DPI)

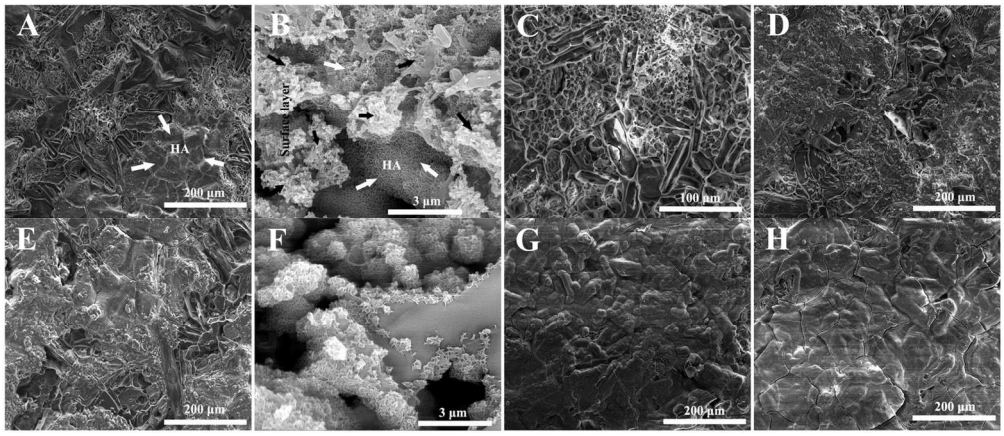

Figure 4 SEM images of the surface morphology of (A, B) Na/0.1Zn-CS disk, (C) Na/0.05Zn-CS disk and (D) Na/0.025Zn-CS disk after being soaked in SBF for 1 week; SEM images of (E) the surface morphology of Na/0.1Zn-CS disk, (F) the wall of the pores in the surface of Na/0.1Zn-CS disk, the surface morphology of (G) Na/0.05Zn-CS disk and (H) Na/0.025Zn-CS disk after being soaked in the SBF solution for 2 weeks. The black arrows in B indicate the original (Zn, Na)-containing layer on the surface of Na/0.1Zn-CS disk, and the white arrows in A and B indicate the deposited Zn/Na co-doped HA layer after Na/0.1Zn-CS disk being soaked in SBF for 1 week.
139x60mm (300 x 300 DPI)

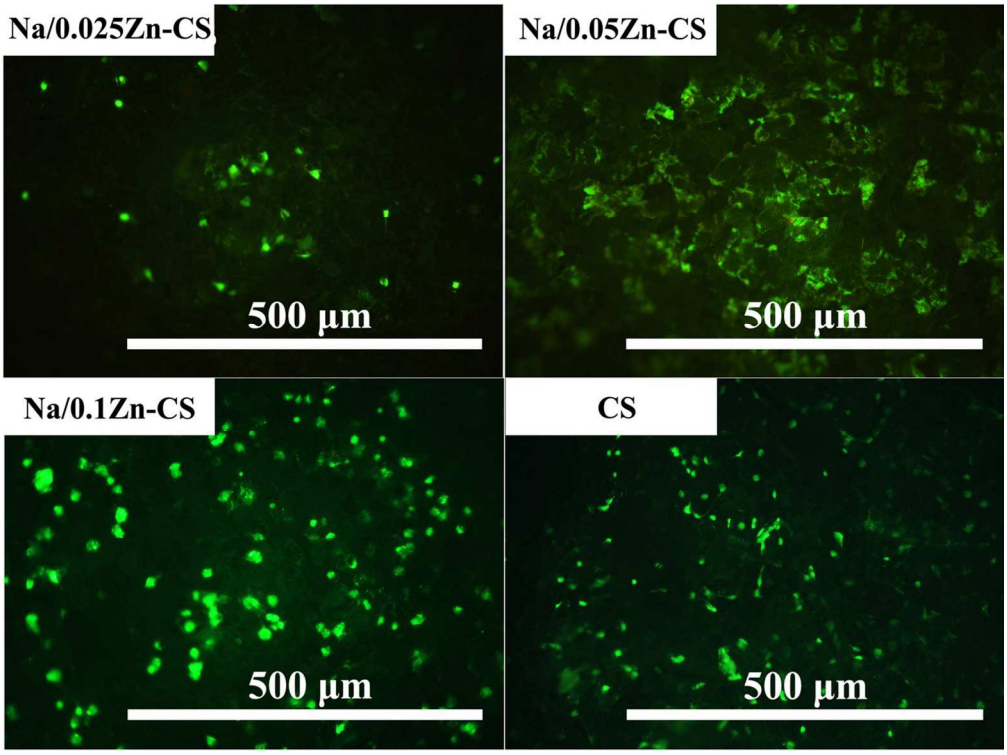

Figure 5 The live cell staining fluorescence images of rBMSCs cultured on the surface of Na/Zn-CS disk and CS disk for 1 day, respectively.
119x89mm (300 x 300 DPI)

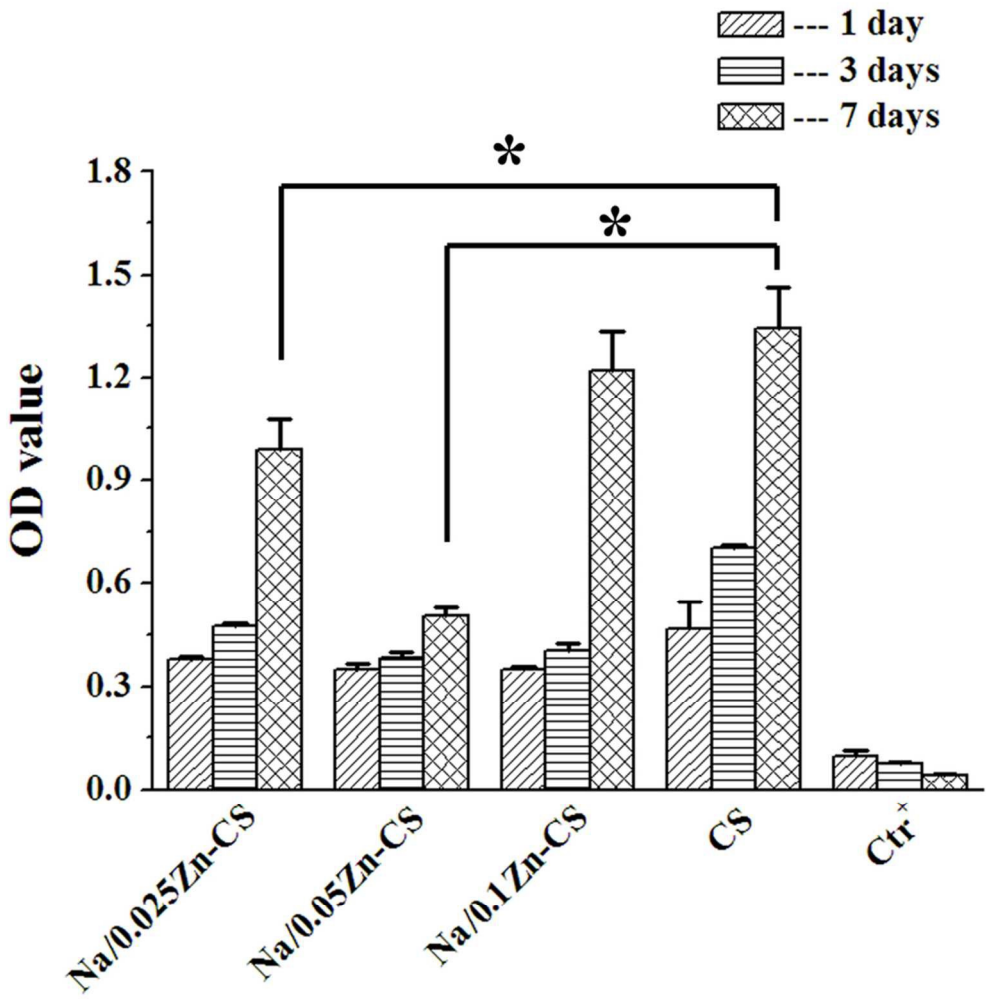

Figure 6 The proliferation of rBMSCs cultured on the surface of Na/Zn-CS disk and CS disk for 1, 3, 7 days, respectively. (n=4) *The Na/Zn-CS group compared with the CS group, P<0.05. CS is used as the control group and 0.64% phenol solutions were used as the positive control (Ctr+).
80x81mm (300 x 300 DPI)

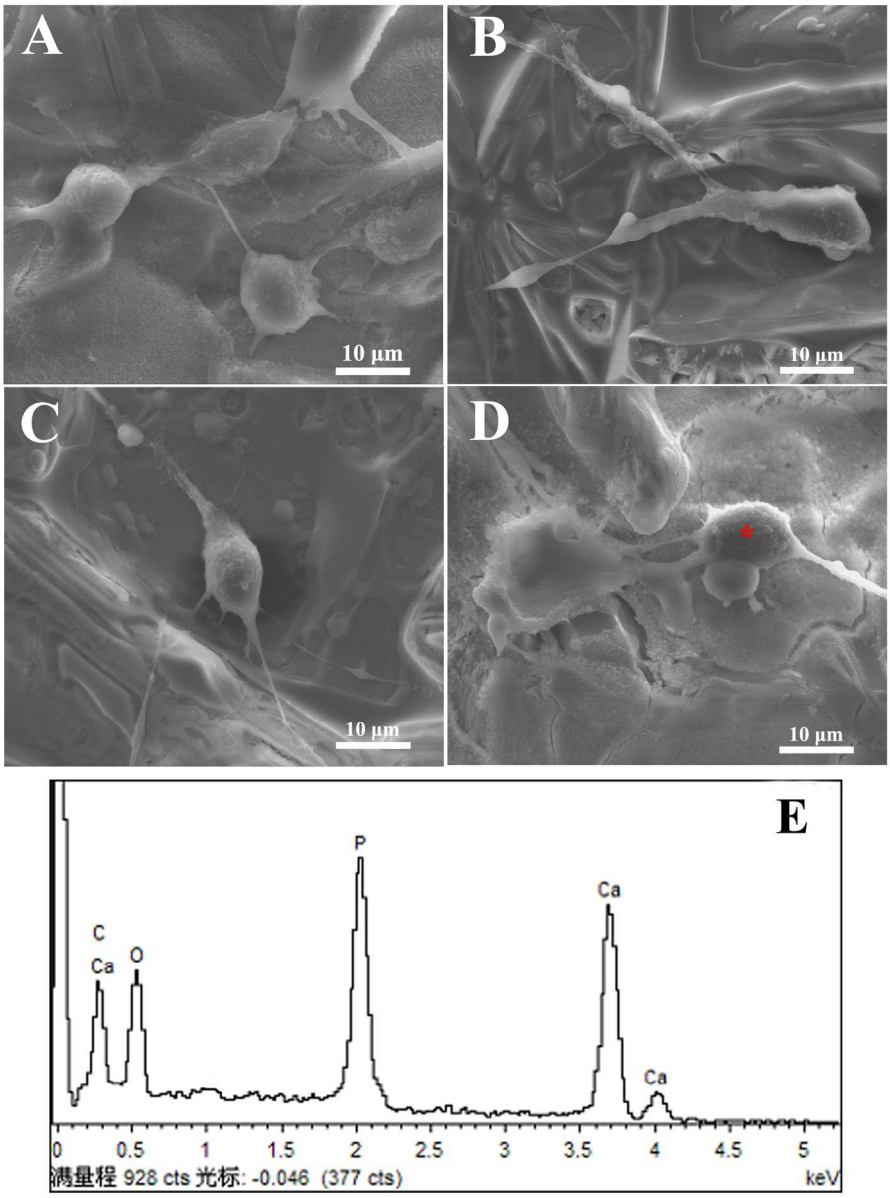

Figure 7 SEM images of rBMSCs attached on the surface of (A) CS disk, (B) Na/0.1Zn-CS disk, (C) Na/0.05Zn-CS disk and (D) Na/0.025Zn-CS disk after being co-cultured for 1 day. (E) EDS test result of the element composition of tiny particles (red *) deposited on the surface of rBMSCs.
218x293mm (300 x 300 DPI)

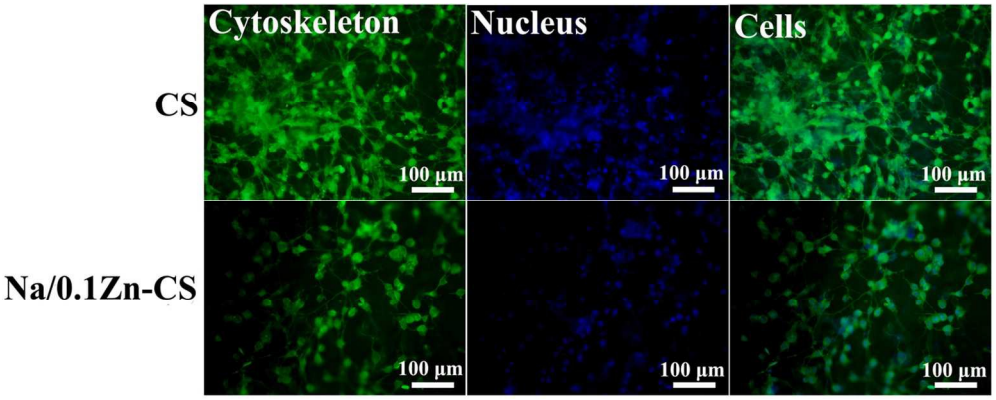

Figure 8 The staining images of F-actin (green, left), nucleus (blue, middle) and their merged images (right) of rBMSCs cultured on the surface of CS disk and Na/0.1Zn-CS disk for 7 days, respectively.
121x47mm (300 x 300 DPI)

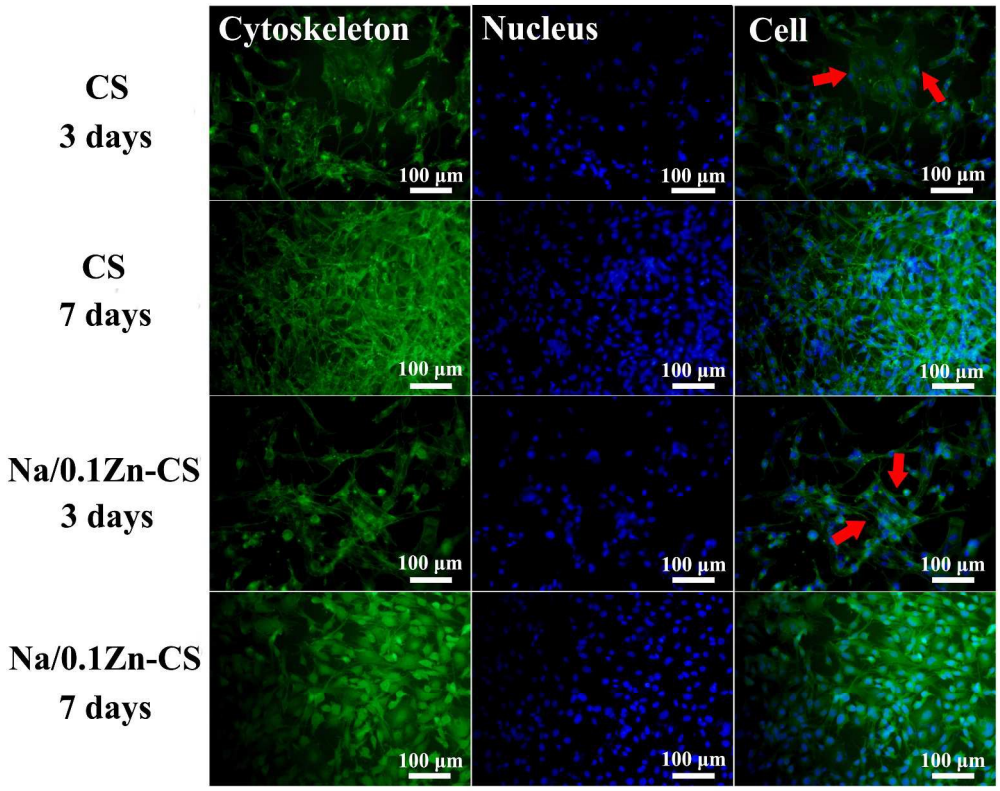

Figure 9 The staining images of F-actin (green, left), nucleus (blue, middle) and their merged images (right) of rBMSCs attached on the 12-well plate when they were co-cultured with CS disks and Na/0.1Zn-CS disk for 3, 7 days, respectively. Red arrows directed region refers to the cytoplasmic meshwork, which was formed by the expanding of the cytoskeleton.
307x241mm (300 x 300 DPI)

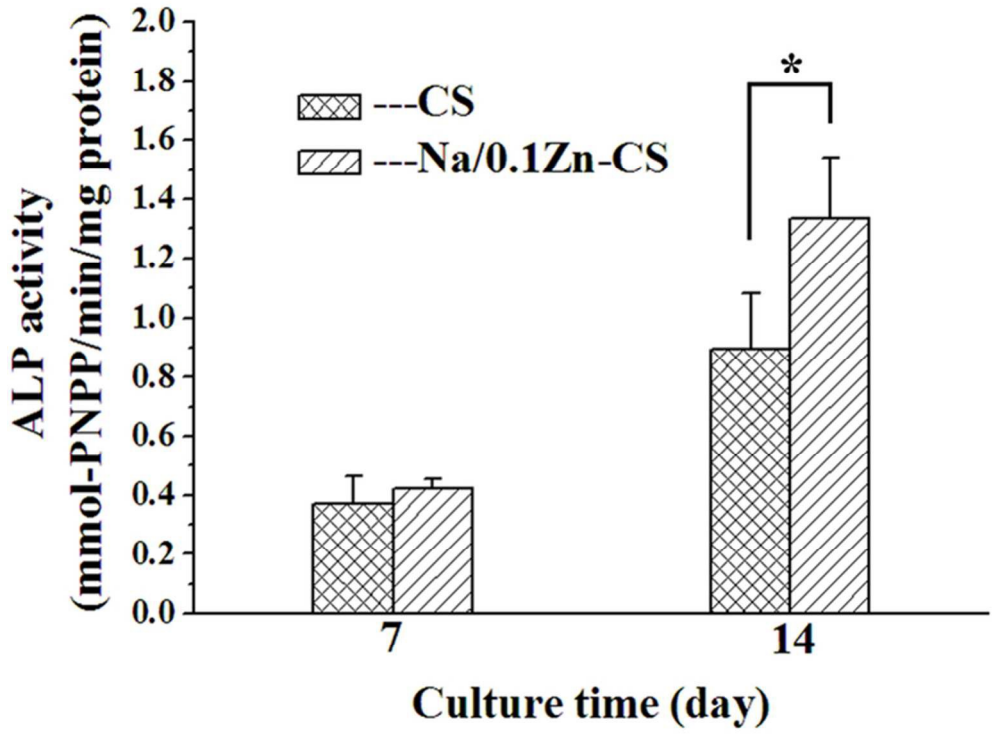

Figure 10 The ALP activities of rBMSCs cultured on the surface of CS disk and Na/0.1Zn-CS disk for 7, 14 days, respectively. (n=4) *The Na/0.1Zn-CS group compared with the pure CS group after the incubation for 14 days, $P<0.05$.
60x46mm (300 x 300 DPI)